coatings

MDPI

Article

Synthesis of Chitosan-Coated $Co_{0.5}Zn_{0.5}Fe_2O_4$ Nanoparticles for Contrast Enhancement in Magnetic Resonance Imaging

Apichaya Worawong * and Wandee Onreabroy *

Department of Physics, Faculty of Science, King Mongkut's University of Technology Thonburi, Bangkok 10140, Thailand

* Correspondence: apichaya.wo@mail.kmutt.ac.th (A.W.); wandee.onr@mail.kmutt.ac.th (W.O.)

Abstract: Magnetic resonance imaging (MRI) is an imaging technique that is widely used for the identification of internal organs, and for the medical diagnosis of tumors and cancer in the body. In general, gadolinium is used as a contrast agent to enhance image contrasting in MRI. In this study, chitosan-coated $Co_{0.5}Zn_{0.5}Fe_2O_4$ nanoparticles were synthesized using a co-precipitation method with a calcination temperature of 500 °C. The nanoparticles were then coated with chitosan and treated under an external magnetic field of 400 mT. X-ray diffractometer results showed that the chitosan-coated $Co_{0.5}Zn_{0.5}Fe_2O_4$ nanoparticles had a pure phase of $Co_{0.5}Zn_{0.5}Fe_2O_4$ at the (3 1 1) plane, with an average particle size of 26 nm. The presence of chitosan on the $Co_{0.5}Zn_{0.5}Fe_2O_4$ nanoparticles was confirmed by Fourier transform infrared spectroscopy, which showed the primary amine and secondary amine functional groups of chitosan. Here, coating the nanoparticle with chitosan not only prevented nanoparticle agglomeration, but also improved the particle surface charge and reduced the particle toxicity for in vivo testing. Vibrating sample magnetometer results showed that the maximum magnetization value of the magnetic field-assisted process was increased to 8.85 emu/g. Finally, chitosan-coated $Co_{0.5}Zn_{0.5}Fe_2O_4$ nanoparticles with 400 mT of magnetic field assistance increased the average brightness in MRI of mouse liver by 21% compared to using gadolinium.

Keywords: cobalt–zinc ferrite; magnetic field-assisted process; magnetic nanoparticles; magnetic resonance imaging

check for updates

Citation: Worawong, A.; Onreabroy, W. Synthesis of Chitosan-Coated $Co_{0.5}Zn_{0.5}Fe_2O_4$ Nanoparticles for Contrast Enhancement in Magnetic Resonance Imaging. *Coatings* **2023**, *13*, 276. https://doi.org/10.3390/coatings13020276

Academic Editors: Marat R. Gafurov and Fengwei (David) Xie

Received: 6 December 2022
Revised: 20 January 2023
Accepted: 21 January 2023
Published: 25 January 2023

Copyright: © 2023 by the authors. Licensee MDPI, Basel, Switzerland. This article is an open access article distributed under the terms and conditions of the Creative Commons Attribution (CC BY) license (https://creativecommons.org/licenses/by/4.0/).

1. Introduction

Magnetic nanoparticles are used in magnetic separation, catalysts, drug delivery [1], hyperthermia therapy [2] and magnetic resonance imaging (MRI) [3,4]. In clinical practice, MRI contrast agents are divided into two parts, T_1 and T_2 agents. T_1 agents, such as the paramagnetic metal gadolinium (Gd^{3+}) type, can alter the longitudinal (T_1) relaxation times of water protons to produce a bright positive signal intensity in images, and increase the clarity of cells. The Dotarem brand drug is a gadolinium-based contrast agent frequently used in MRI. All obtainable gadolinium-based contrast agents are chelates that contain the gadolinium ion (Gd^{3+}). The gadolinium parts of the lanthanide group of elements are high in toxicity due to free gadolinium. The T_1 relaxivity of gadolinium is 4.2 L/mmol s^{-1} in blood [5]. T_2 agents, such as superparamagnetic iron oxide nanoparticles (SPION), are used to alter the transverse (T_2) relaxation times of water protons. T_2 agents provide a dark negative signal intensity in images, and can be used to visualize stem cells grafted in organs that appear as high signal intensity. In practice, T_2 agents appear to be a preferent MRI contrast agent for monitoring internal organs due to their high sensitivity and excellent biocompatibility [4]. Therefore, in this research, we focused on the synthesis of superparamagnetic-based nanoparticles as the T_2 agent. The diameters of some metals and metal oxide nanoparticles, which exhibit superparamagnetic properties, are as small as 10–20 nm [6]. When a superparamagnetic is placed under an external magnetic field, the magnetic moment is aligned with the external magnetic field's. However, without an

external magnetic field, a superparamagnetic has zero magnetization values, similar to those of paramagnets [6,7].

There are many methods for the preparation of superparamagnetic nanoparticles, such as co-precipitation [8], sol-gel [9], hydrothermal [10], ball milling, combustion [11], etc. However, the most reasonable method for the synthesis of superparamagnetic nanoparticles is co-precipitation, due to its ease of production on a large scale, its crystallite-size adjustment and magnetization value control. Previously, it was also reported that the co-precipitation method, with the help of an external magnetic field, could enlarge the unit cell size and enhance the saturation magnetization (M_s), remanence magnetization (M_r) and coercivity (H_c) of the nanoparticles [12–14]. There are many types of superparamagnetic nanoparticles, e.g., Fe_3O_4 [15], $CoFe_2O_4$ [12] and $Co_xZn_yFe_2O_4$ [16]. Among these nanomaterials, $Co_xZn_yFe_2O_4$ seems to be the most interesting material, as it provides the highest M_s and M_r, which are good for contrast enhancement in MRI. However, $Co_xZn_yFe_2O_4$ nanoparticles are intrinsically toxic to living organisms; therefore, coating the particles with a biocompatible material is crucial. There have been many materials used to coat $Co_xZn_yFe_2O_4$ nanoparticles, such as dextrin [17], silica [18] and polyethylene glycol (PEG) [19].

Currently, there are several studies related to the synthesis of magnetic nanoparticles that have been applied to medical applications. Dextran-coated $Co_{0.8}Zn_{0.2}Fe_2O_4$ nanoparticles were synthesized using the heat treatment method, in order to improve the received MRI signals as a result of the quality of tissue relaxation [20]. Moreover, dimercaptosuccinic acid (DMSA)-coated $Co_{0.6}Zn_{0.4}Fe_2O_4$ nanoparticles were synthesized using the thermal decomposition method for use as suitable contrast agents for both T_2- and T_2*-weighted MRI in an in vivo study of rat liver [21]. Sattarahmady et al. [17] showed that the relaxivity of dextrin-coated $Zn_{0.5}Co_{0.5}Fe_2O_4$ nanoparticles was 79 $mM^{-1}{\cdot}s^{-1}$ with 1.5 T of MRI. They also found that dextrin-coated $Zn_{0.5}Co_{0.5}Fe_2O_4$ nanoparticles offered an M_s value of 24 emu/g. However, its H_c value (17 emu/g) was still too high to be a superparamagnetic material. Moreover, Ahmad et al. [18] reported that silica-coated $Co_{0.6}Zn_{0.4}Fe_2O_4$ nanoparticles provided a suitable M_s value for MRI. The transverse relaxivity (T_2) of the nanoparticles was 126.86 $mM^{-1}{\cdot}s^{-1}$ in 4.7 T of MRI. Moreover, polyethylene glycol (PEG)-coated Gd_2O_3, which has high paramagnetic properties, is suitable for use in medical applications. Gadolinium oxide (Gd_2O_3) has been studied in the development of radiothermal combined cancer therapies, due to the high longitudinal relaxation rate of Gd_2O_3 as the imaging agent [22].

Examples of the research related to cobalt–zinc ferrite ($Co_{1-x}Zn_xFe_2O_4$) nanoparticle synthesis via different methods for medical application are shown in Table 1.

Table 1. Literature review of synthesis methods for cobalt–zinc ferrite ($Co_{1-x}Zn_xFe_2O_4$) and features.

Synthesis	Method	Particle Sizes (nm)	Magnetic Properties	Applications	Ref.
Dextrin-coated $Co_{0.5}Zn_{0.5}Fe_2O_4$	Co-precipitation	3.9	Superparamagnetic	MRI contrast agent	[17]
Silica-coated $Co_{0.6}Zn_{0.4}Fe_2O_4$	Hydrothermal technique	90	Superparamagnetic	MRI contrast agent and magnetic hyperthermia	[18]
Dextran-coated $Co_{0.8}Zn_{0.2}Fe_2O_4$	Heat treatment method	34	Superpara-magnetic	MRI contrast agent	[20]
DMSA-coated $Co_{0.6}Zn_{0.4}Fe_2O_4$	Thermal decomposition method	8	Superpara-magnetic	MRI contrast agent	[21]

The medical applications of magnetic nanoparticles are still being developed for use in the diagnosis and treatment of tumors and cancer. This research is focused on synthesizing chitosan-coated $Co_{0.5}Zn_{0.5}Fe_2O_4$ nanoparticles with superparamagnetic properties and a high magnetization value from being treated with 400 mT of magnetic field assistance. Chitosan coating not only increases the dispersion of magnetic particles, but also has no

toxicity. This has led to the application of chitosan-coated $Co_{0.5}Zn_{0.5}Fe_2O_4$ nanoparticles assays to mice in the study of MRI imaging contrast enhancement. Chitosan is non-toxic because of its hydrophilic amino groups, biocompatibility, high responsiveness to chemical modification, high water permeability and cost effectiveness. Therefore, chitosan has been used to coat nanometer-sized materials for biomedical applications such as biosensors, drug delivery and magnetic resonance imaging (MRI) [23]. Magnetic nanoparticle research in the medical field continues to challenge particle size control, particle agglomeration reduction, non-toxicity and optimum magnetic values [24].

In this research, $Co_{0.5}Zn_{0.5}Fe_2O_4$ nanoparticles synthesized using the co-precipitation method with the help of an external magnetic field (400 mT) were reported. The contents of zinc ions and the calcine temperature were varied and investigated. The particles were then coated with chitosan to improve their biocompatibility. The chitosan-coated particles were characterized via X-ray powder diffractometer (XRD), transmission electron microscopy (TEM), Fourier transform infrared spectroscopy (FTIR), vibrating sample magnetometer (VSM) and acute toxicity testing for their crystal structure, particle size, chemical functionalized groups, magnetic properties and biocompatibility, respectively. The chitosan-coated nanoparticles were then applied for MRI usage in animal testing.

2. Materials and Methods

2.1. Synthesis of Chitosan-Coated $Co_{0.5}Zn_{0.5}Fe_2O_4$

Cobalt–zinc ferrite ($Co_{0.5}Zn_{0.5}Fe_2O_4$) nanoparticles were synthesized using the co-precipitation method and mixed with cobalt (II) nitrate ($Co(NO_3)_2{\cdot}6H_2O$), zinc (II) nitrate ($Zn(NO_3)_2{\cdot}6H_2O$) and iron(III) nitrate ($Fe(NO_3)_3{\cdot}9H_2O$), whose reagent grades were 98%; they were purchased from Sigma-Aldrich (Saint Louis, MI, USA). This mixture powder was stirred at 80 °C for 60 min. Next, sodium hydroxide (NaOH) was gradually added to the precipitate and stirred up to 80 °C for 30 min. Subsequently, the precipitated powders were washed with acetone at a calcine temperature of 200 °C to remove moisture, carbonaceous matter and all remaining substances of the oxides. The powders were then calcined at a temperature of 500 °C for 2 h (rate 3 °C/min), and received $Co_{0.5}Zn_{0.5}Fe_2O_4$ nanoparticles.

Chitosan-coated $Co_{0.5}Zn_{0.5}Fe_2O_4$ nanoparticles were prepared by adding 2% chitosan with 1% acetic acid in 50 mL of deionized water. Next, the sample was sonicated for 30 min and centrifuged at 2500 rpm for 10 min, and then at 3500 rpm for 15 min. Finally, the chitosan-coated $Co_{0.5}Zn_{0.5}Fe_2O_4$ nanoparticles were deposited into a plastic tube and treated under 400 mT of magnetic field assistance in the same easy direction for 20 min. The chitosan-coated $Co_{0.5}Zn_{0.5}Fe_2O_4$ nanoparticles were placed between magnetic-fielded iron platforms from an induction coil wrapped around the iron platforms with direct electric current. The direction of the magnetic field moving from the lower to the upper iron platform ($\vec{H}$) is shown in Figure 1, which is the same direction as the magnetic field from the north pole to the south pole.

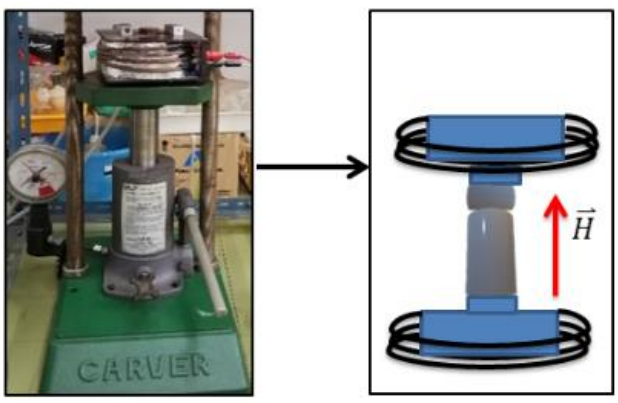


Figure 1. An instrument used to modify compression under the magnetic field-assisted process, and a magnetic field direction simulation.

2.2. Characterization

The crystal structure and phases of $Co_{0.5}Zn_{0.5}Fe_2O_4$ with 400 mT of magnetic field assistance were characterized with an XRD (Rigaku, Austin, TX, USA) X-ray powder diffractometer using Cu K-α (λ = 1.544 Å). The crystallite sizes of the nanocrystalline samples were measured with X-ray line-broadening analyses using the Debye–Scherrer formula. The morphologies and particle sizes of the chitosan-coated $Co_{0.5}Zn_{0.5}Fe_2O_4$ nanoparticles were examined using transmission electron microscopy (TEM, JEOL-JEM-2100 Plus, Tokyo, Japan). The chemical composition of the chitosan coating was studied with Fourier transform infrared spectroscopy (FTIR, Perkin Elmer System 2000, Waltham, MA, USA) absorption bands using KBr pellets in the range of 500–4000 cm^{-1}. Their magnetic properties were measured at room temperature with a vibrating sample magnetometer (VSM) within the magnetic field of ±8.5 kOe.

2.3. Biocompatibility

The chitosan-coated $Co_{0.5}Zn_{0.5}Fe_2O_4$ nanoparticles were tested for acute toxicity in Wistar rats using the International Organization for Standardization (ISO 10993-11) biological evaluation of medical devices part 11 test for systemic toxicity 2017 (ethics committee name: National Laboratory Animal Center, Mahidol University, approval code: non-GLP2019-22, approval date: 24 September 2019).

This study was handled by Jiraporn Tangthong, study director at the National Laboratory Animal Center (NLAC), Mahidol University. Wistar rats are often used in studies and research in various fields, such as nutrition, pathology, pharmacology and physiology.

Source of animals: The animals were reserved from the Animal Production Office, National Laboratory Animal Center, Mahidol University, Nakhon Pathom, Thailand, recorded on the "Laboratory Animal Reservation Checklist" according to the "Laboratory Animal Reservation, Receiving and Management" standard operating procedure, SOP-G.RA-059, and recorded on the "Laboratory Animal Reservation Checklist" work sheet, F-G.RA-059/02.

Animal welfare: Guidelines from the Guide for the Care and Use of Laboratory Animals (Institute of Laboratory Animal Resources, National Academic Press 2011; 8th edition NIH publication number #85–23, revised 2011) were strictly followed throughout the study. The study was approved by the National Laboratory Animal Center Animal Care and Use Committee (NLAC-ACUC), Mahidol University, Thailand.

Housing conditions: The animals were housed in the Experimental Building (Building 7), Animal 1, Mini Room 3. The mini room was used according to the "Operation and Maintenance of Mini Room" standard operating procedure, SOP-E.RA-004, and recorded on the "Mini Room Use Log" work sheet, F-E.RA-004/01. The conditions were as follows: temperature 22 ± 3 °C; humidity 30–70%; and standard fluorescent light, 12:12 (light:dark). The temperature and humidity in the mini room was measured daily by data logger and recorded on the "Environmental Monitoring Record" work sheet, F-G.RA-025/05.

Gross necropsy: All animals in the systemic toxicity study were subjected to a full, detailed gross necropsy, which included careful examination of the external surface of the body and all orifices, along with the cranial, thoracic and abdominal cavities and skin layer.

The experiment used 20 female Wistar rats that were divided into three groups. Group 1 (five rats) were injected with normal saline for control items. Group 2 (five rats) were injected with 0.1 mL of chitosan-coated $Co_{0.5}Zn_{0.5}Fe_2O_4$. Only group 1 and group 2 were tested at first, in order to reduce the number of rat deaths. The last group of 10 rats were injected with 0.1 mL of chitosan-coated $Co_{0.5}Zn_{0.5}Fe_2O_4$. After injection, all of the rats were observed at 4, 24, 48 and 72 h.

2.4. Animal Testing

The animal testing of chitosan-coated $Co_{0.5}Zn_{0.5}Fe_2O_4$ in MRI was conducted in collaboration with the Advanced Diagnostic Imaging Center (AIMC), Faculty of Medicine Ramathibodi Hospital. The consultant radiologist was Witaya Sungkarat and the veterinar-

ian was Coopet Nitsakulthong, from Chulalongkorn University Laboratory Animal Center. $Co_{0.5}Zn_{0.5}Fe_2O_4$ nanoparticles were studied to enhance contrast agents by Intera Achieva 3 T (Philips) (ethics committee name: Advanced Diagnostic Imaging Center (AIMC), Faculty of Medicine Ramathibodi Hospital, approval code: 001/2562, approval date: 6 February 2019).

The experimental design for animal testing with MRI used Mlac:ICR (Mus musculus) females, 17–24 g and aged 4–5 weeks.

Housing conditions: The Mlac:ICR was housed in a controlled environment. The ventilation, temperature and humidity were controlled by an HVAC (heating, ventilating, air conditioning) system. The temperature range was controlled at approximately 22 ± 2 °C. The relative humidity range was approximately 55 + 10%. Air changes per hour were 15–20 ACH. The light:dark cycle was adjusted to 12:12 h. Mice are sensitive to noise, so the noise level was maintained at <85 db.

The experimental design for the animal testing of chitosan-coated $Co_{0.5}Zn_{0.5}Fe_2O_4$ in MRI was divided into four conditions. All mice were injected with Zoletil 40 mg/kg and Xylazine 2 mg/kg. In the first condition, the mouse was normal, without any substances. In the second condition, the mouse was injected with 0.01 mL of gadolinium. In the third condition, the mouse was injected with 0.01 mL of chitosan-coated $Co_{0.5}Zn_{0.5}Fe_2O_4$ nanoparticles. In the last condition, the mouse was injected with 0.01 mL of chitosan-coated $Co_{0.5}Zn_{0.5}Fe_2O_4$ nanoparticles with 400 mT of external magnetic field assistance.

3. Results and Discussion

3.1. Material Characterization

The crystal structure, phase and crystallite size of chitosan-coated $Co_{0.5}Zn_{0.5}Fe_2O_4$ nanoparticles with magnetic field assistance (400 mT) were investigated using XRD. The XRD peaks of the chitosan-coated $Co_{0.5}Zn_{0.5}Fe_2O_4$ nanoparticles with 400 mT of magnetic field assistance matched with those of the cobalt–zinc ferrite phase (Figure 2). The (2 2 0), (3 1 1), (2 2 2), (4 0 0), (4 2 2), (5 1 1) and (4 4 0) planes corresponded to spinel ferrites with cubic symmetry, demonstrating the formation of the $Co_{0.5}Zn_{0.5}Fe_2O_4$ phase. The strongest peak was the (3 1 1) plane growth along this direction, and every peak matched JCPDF file no. 80-6488 for $Co_{0.5}Zn_{0.5}Fe_2O_4$. The average crystallite size was estimated using the Debye–Scherrer equation (Equation (1)) from full-width at half maximum; FWHM of the (3 1 1) plane:

$$D = \frac{0.9\lambda}{\beta \cos\theta} \quad (1)$$

where D is the average crystallite size, β represents full width at half maximum of peaks and θ denotes the Bragg's angle [25]. The chitosan-coated $Co_{0.5}Zn_{0.5}Fe_2O_4$ nanoparticles with magnetic field assistance (400 mT) were approximately 12 nm, whereas zinc ion x = 0.5 had a small crystallite size of approximately 10–17 nm because the Zn^{2+} ions were not completely the normal spinel, and the Co^{2+} ions transferred to the tetrahedral sites [26]. However, zinc ions less than x = 0.5 mostly occupied the tetrahedral sites, but zinc ions more than x = 0.5 gradually occupied octahedral sites. Therefore, the lattice parameter increased with the Zn content. The variation in the ionic size of Co^{2+} (0.72 Å) was lower than that of Zn^{2+} (0.74 Å) [27]. Accordingly, the study of the $Co_{1-x}Zn_xFe_2O_4$ (x = 0.0 and 0.5) nanoparticles confirmed the spinel cubic ferrite structure [28]. In agreement with the research, the $Co_{1-x}Zn_xFe_2O_4$ (x = 0.0 to 0.5) nanoparticles were prepared using the microwave combustion method [27]. The XRD patterns confirmed the formation of a single-phase $CoFe_2O_4$ inverse spinel structure without impurities. The lattice parameter increased from 8.380 to 8.396 Å with an increasing Zn^{2+} fraction.

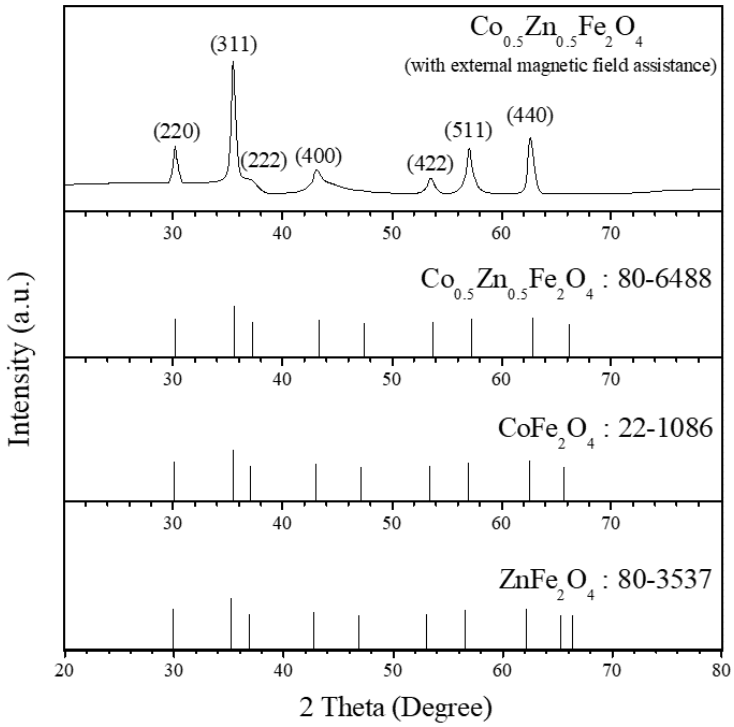


Figure 2. Indexed X-ray diffraction pattern for chitosan-coated $Co_{0.5}Zn_{0.5}Fe_2O_4$ nanoparticle calcined powders at 500 °C with 400 mT of magnetic field assistance.

When comparing the XRD pattern, other studies with magnetic field-assisted processes found no change in all peaks. The XRD pattern of cobalt ferrite nanoparticles was synthesized using the combustion method, with a 1 T magnetic field-assisted compaction process that resulted in a pure cubic spinel phase. Every peak matched JCPDF file no. 22-1086 for cobalt ferrite, before and after applying the magnetic field-assisted compaction process [25]. Furthermore, the study of $CoFe_2O_4$ nanoparticles using the reverse co-precipitation method with alternative magnetic field assistance showed that the XRD patterns of all samples indicated no phase impurity, and that all peaks were attributed to the cubic symmetry spinel, and applying the magnetic field could change the structure [12]. In addition, in Rietveld analysis, the increased applied magnetic field affected more reverse spinel structures. The magnetic field-assisted process affected the increase in crystallite size and the occupation of Co^{2+} in the octahedral site of $Co_{0.5}Zn_{0.5}Fe_2O_4$ nanoparticles, as shown using the Rietveld method. The higher Co^{2+} (0.0745 nm) occupied the octahedral site, with a higher ionic radius in the magnetic field-assisted process. Related magnetite research improved the magnetic properties and crystallinity via the magnetic field-assisted process from the Lorentz force reaction. The crystallite sizes of the $Co_{0.5}Zn_{0.5}Fe_2O_4$ nanoparticles were controlled by adjusting the partial substitution of zinc, calcine temperature, pH value and rate of ferrite formation. The particles sizes and maximum magnetization values are hereby discussed in terms of TEM and VSM, respectively.

The morphology of the particles was characterized using TEM, and the particle size was measured with the Image-Pro Plus software. The chitosan-coated $Co_{0.5}Zn_{0.5}Fe_2O_4$ nanoparticles at a calcine temperature of 500 °C and an applied magnetic field of 400 mT were spherical shapes, with an average core size of 26 ± 1.86 nm (Figure 3a,b) and a chitosan thickness of approximately 2 nm (Figure 3c). Uniform $Co_{0.5}Zn_{0.5}Fe_2O_4$ nanoparticles may be convenient for attaching the negative charge of target cells or cancer cells. The existence of the chitosan coating on the surface of $Co_{0.5}Zn_{0.5}Fe_2O_4$ was confirmed via FTIR.

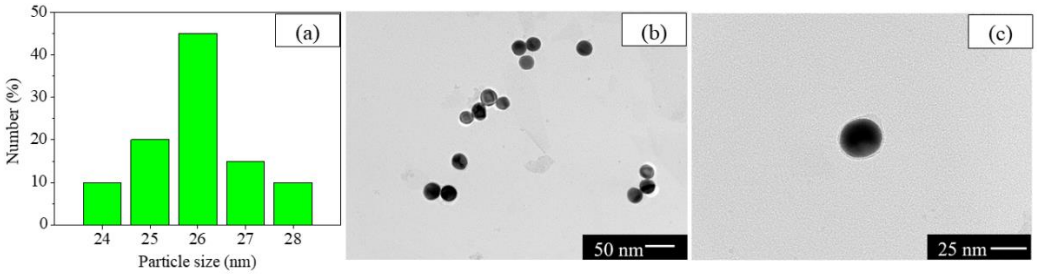


Figure 3. TEM images and a histogram image (**a**) of chitosan-coated $Co_{0.5}Zn_{0.5}Fe_2O_4$ nanoparticles with 400 mT of external magnetic field assistance at a magnification of (**b**) ×100,000 and (**c**) ×250,000.

The FTIR spectra of chitosan-coated $Co_{1-x}Zn_xFe_2O_4$ with x = 0.1, 0.5 and 0.9 nanoparticles at 500 °C had hydroxyl groups at wavenumbers 3440 to 3220 cm^{-1} and 1650 to 1630 cm^{-1} from water (Figure 4), and metal–oxygen bonds at 610 to 580 cm^{-1} and 440 to 410 cm^{-1} [8]. Chitosan coating showed the primary amine at 3410 cm^{-1} and the secondary amine at 1654 cm^{-1}. Consequently, the wavenumber 3410 cm^{-1} was defined as the OH-stretching vibration of pure chitosan [29]. FTIR measurements were carried out on all three samples to confirm the same chitosan coating results. The FTIR spectra of chitosan-coated $Co_{1-x}Zn_xFe_2O_4$ with x = 0.1, 0.5 and 0.9 nanoparticles showed the presence of primary amine and secondary amine from chitosan. The chitosan coating of the $Co_{0.5}Zn_{0.5}Fe_2O_4$ nanoparticles needed to be checked first, in order to ensure that the particles were well dispersed with the functional groups of chitosan coating before treatment with 400 mT of magnetic field assistance. The magnetic properties of the chitosan-coated $Co_{0.5}Zn_{0.5}Fe_2O_4$ nanoparticles with 400 mT of magnetic field assistance were measured using VSM analysis.

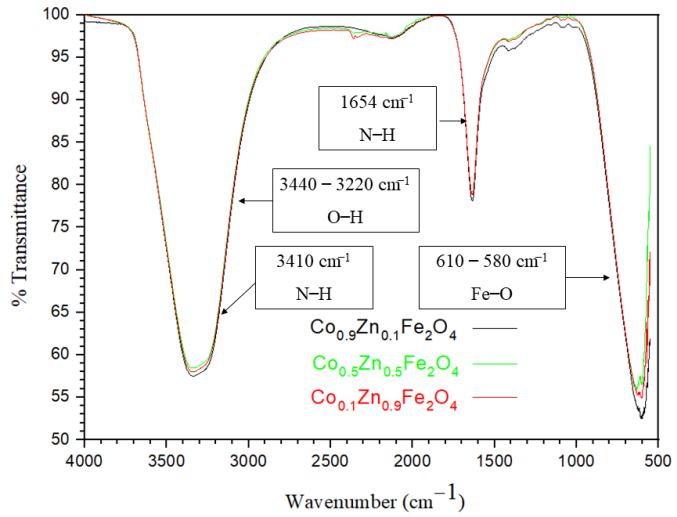


Figure 4. Fourier transform infrared spectroscopy (FTIR) spectra of chitosan-coated $Co_{1-x}Zn_xFe_2O_4$ with x = 0.1, 0.5 and 0.9 nanoparticles at a calcine temperature of 500 °C.

The magnetic properties of chitosan-coated $Co_{0.5}Zn_{0.5}Fe_2O_4$ nanoparticles (with and without 400 mT of external magnetic field assistance) were compared with those of a commercial drug (Gd from Dotarem®) (Figure 5). The M_m and H_c values of the chitosan-coated $Co_{0.5}Zn_{0.5}Fe_2O_4$ nanoparticles with 400 mT of magnetic field assistance (red line, Figure 5) were 8.85 emu/g and 1.41 Oe, respectively. The high M_m and low H_c values of the chitosan-coated $Co_{0.5}Zn_{0.5}Fe_2O_4$ nanoparticles with 400 mT of magnetic field assistance indicated that their magnetic properties are close to those of superparamagnetic material. In addition, the M_m and H_c values of the chitosan-coated $Co_{0.5}Zn_{0.5}Fe_2O_4$ nanoparticles without the 400 mT of magnetic field assistance (green line, Figure 5) were approximately 7.39 emu/g and 140 Oe, respectively. Here, the H_c value was too high for superparamag-

netic material. Moreover, the results showed that the M_m of Gd from Dotarem® was very low at 0.08 emu/g (pink line, Figure 5), because of its paramagnetic characteristics. The chitosan-coated $Co_{0.5}Zn_{0.5}Fe_2O_4$ nanoparticles with 400 mT of magnetic field assistance were studied for acute toxicity in laboratory animals to confirm their biocompatibility.

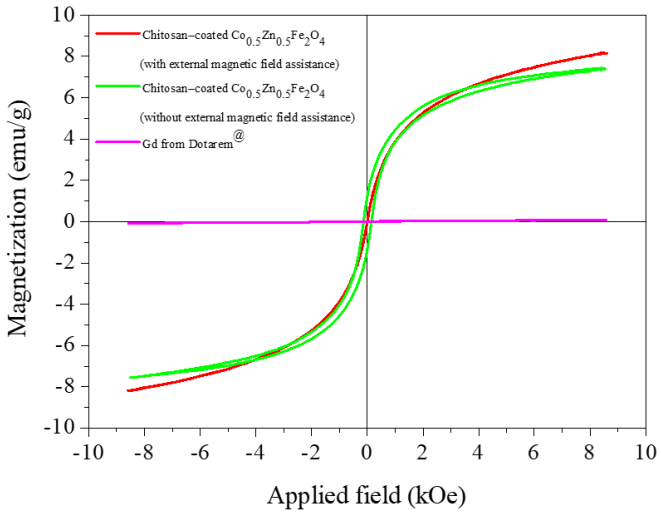


Figure 5. Room temperature magnetization curve of chitosan-coated $Co_{0.5}Zn_{0.5}Fe_2O_4$ nanoparticles (with and without 400 mT of external magnetic field assistance) and Gd from Dotarem® (Guerbet, Roissy CdG Cedex, France).

3.2. Biocompatibility Study

The bodyweight of the Wistar rats injected with the chitosan-coated $Co_{0.5}Zn_{0.5}Fe_2O_4$ nanoparticles increased along the same trend as that of the control group (Figure 6). This implied that the control group and the nanoparticle-injected groups had no differences in biological responses, no abnormal symptoms and no deaths. After the gross necropsy of all the Wistar rats, there were no changes found in the macroscopic examination of all organs. These results were in agreement with a previous report stating that the biocompatibility of $Co_{0.5}Zn_{0.5}Fe_2O_4$ nanoparticles was up to 70% of mean cell viability at concentrations of 0.05 g/mL [30].

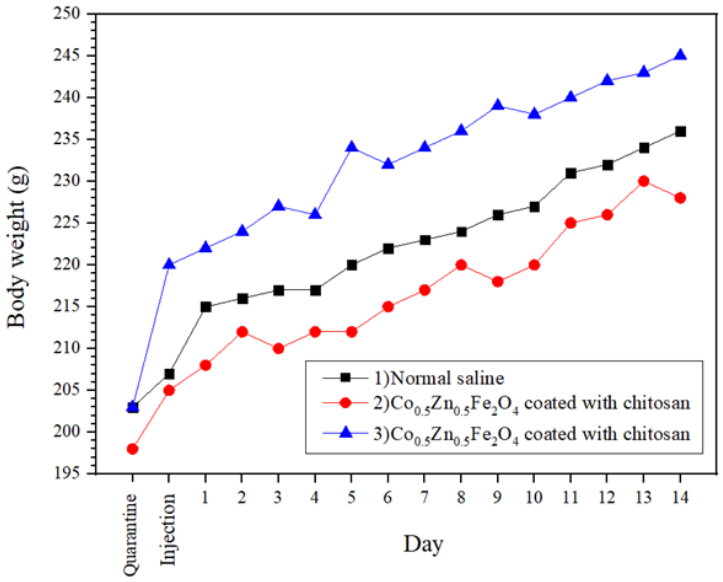


Figure 6. Wistar rat body weight changes in acute systemic toxicity with chitosan-coated $Co_{0.5}Zn_{0.5}Fe_2O_4$ nanoparticles.

Thus, the chitosan-coated $Co_{0.5}Zn_{0.5}Fe_2O_4$ nanoparticles with 400 mT of magnetic field assistance did not affect acute systemic toxicity in Wistar rats. Therefore, chitosan-coated $Co_{0.5}Zn_{0.5}Fe_2O_4$ nanoparticles with 400 mT of magnetic field assistance can be used for MRI imaging in animal testing.

3.3. MRI Application

Typical studies of visceral MRI images require a magnetic resonance monitor with a high magnetic field strength of 3 tesla or higher, so that detailed and high-definition images can be distinguished, and slight differences in the tissues are evident. This requires a minimum of three weighted images, including T_1, T_2 and proton density-weighted (PDW) images, and must be interpreted by a skilled radiologist. T_1 is an anatomy scan because the boundaries of tissues can be clearly distinguished. Fluid is black, solid organs and muscles are gray, but fat is bright. However, T_2 is a pathology scan because the area of fluid collection or edematous tissue is more prominently bright compared with nearby tissues. T_2 is a specific property of each tissue type, with the number of protons present in different tissues with different T_2 values; for example, lipid core, fibrous cap, normal tissue and calcium have T_2 values of 28.1 ms, 51.2 ms, 48.2 ms and 52 ms, respectively. Therefore, the image of the T_2 value map is of the fat pad. Therefore, it may be possible to classify the components inside the fat pad, which is different from the old method that relied on the advantage difference from the intensity of the signal on the image (image intensity contrast) [31].

Gadolinium decreased the T_1 and T_2 values of the neighboring water protons. These effects increased the signal intensity of the T_1-weighted images but reduced the signal intensity of the T_2-weighted images. Lower gadolinium was associated with T_1 shortening, but higher gadolinium concentrations resulted in T_2 shortening. The amount of gadolinium must be controlled to reduce the risk of toxicity in the human body. Examples of magnetic substances used to enhance contrasts in MRI include high-spin manganese (II) and superparamagnetic iron oxide, which greatly affected the T_2 relaxation [32].

The chitosan-coated $Co_{0.5}Zn_{0.5}Fe_2O_4$ nanoparticles at a calcine temperature of 500 °C were pure phase, small particle size, high M_m value and low H_c value, as a result of the improvement in their magnetic properties via the magnetic field-assisted process. Moreover, the chitosan coating increased the distribution of the particles, and it was safety tested for acute toxicity in mice. Therefore, the $Co_{0.5}Zn_{0.5}Fe_2O_4$ nanoparticles were used in an MRI application to test the ability of the contrast agents. The study compared the MRI images of normal mice injected with gadolinium and chitosan-coated $Co_{0.5}Zn_{0.5}Fe_2O_4$ nanoparticles without external magnetic field assistance, with those of chitosan-coated $Co_{0.5}Zn_{0.5}Fe_2O_4$ nanoparticles with 400 mT of external magnetic field assistance. The mean contrast from mice liver using a 3D technique was echo time (TE) = 22 ms and repetition time (TR) = 350 ms. The mean contrast was the average brightness of the organs we studied compared with the total of the MRI images. The mean of normal mice was 406.29 per area of 82 mm^2 (Figure 7a) when the injection of gadolinium was 664.11 per area of 79 mm^2 (Figure 7b). However, the mean of chitosan-coated $Co_{0.5}Zn_{0.5}Fe_2O_4$ nanoparticles without external magnetic field assistance injected to mice was 490.82 per area of 147 mm^2 (Figure 7c). Moreover, chitosan-coated $Co_{0.5}Zn_{0.5}Fe_2O_4$ nanoparticles with 400 mT of external magnetic field assistance injected increased the mean of contrast to 808.18 per area of 82 mm^2 (Figure 7d). However, this study did not increase the concentration of the substance to find the T_1 and T_2 values; therefore, we could not calculate the relaxivity values of the chitosan-coated $Co_{0.5}Zn_{0.5}Fe_2O_4$ nanoparticles.

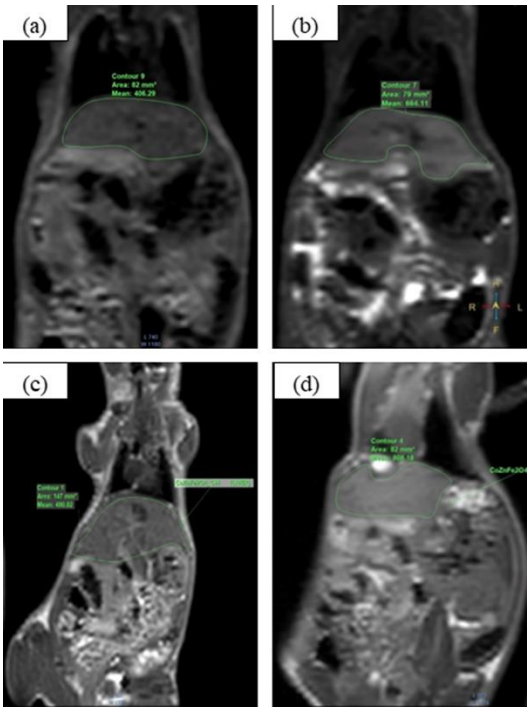


Figure 7. Three-dimensional MRI images of mice liver from (**a**) normal mice; (**b**) mice injected with gadolinium; (**c**) mice injected with chitosan-coated $Co_{0.5}Zn_{0.5}Fe_2O_4$ nanoparticles without external magnetic field assistance; and (**d**) mice injected with chitosan-coated $Co_{0.5}Zn_{0.5}Fe_2O_4$ nanoparticles with 400 mT of external magnetic field assistance. In Supplementary Materials you can find the whole MRI measurement (Video S1) of mice liver from (**a**) normal mice (**left**), (**b**) mice injected with chitosan-coated $Co_{0.5}Zn_{0.5}Fe_2O_4$ nanoparticles with 400 mT of external magnetic field assistance (**middle**), (**c**) mice injected with chitosan-coated $Co_{0.5}Zn_{0.5}Fe_2O_4$ nanoparticles without external magnetic field assistance (**right**); and Video S2 of mice liver from (**b**) both mice injected with gadolinium.

However, research related to silica-coated $Co_{0.6}Zn_{0.4}Fe_2O_4$ nanoparticles used in 4.7 T of MRI found that r_1 and r_2 were 0.07 and 126.86 $mM^{-1}{\cdot}s^{-1}$, respectively. The value of r_1 was very small compared with r_2, which was a regular spherical magnetic nanoparticle agent [16]. Therefore, the r_2/r_1 ratio had to be reduced while the value of r_1 as positive contrast agents increased [33]. The relaxation time (T_1) of Gd-DOTA from Dotarem® 0.5 mol/l with a metal chelate of 278.3 mg/mL used in 0.47 T of MRI was 4.3 $mM^{-1}{\cdot}s^{-1}$ [34]. The longitudinal relaxivity (r_1) of Dotarem® was 5.14, 3.70 and 3.90 $mM^{-1}{\cdot}s^{-1}$ from 3 T, 7 T and 9.4 T MRI, respectively [35]. Furthermore, a study of the high signal in a T2*-weighted image from implanted cells labeled rat mesenchymal stem cells by silica-coated cobalt zinc ferrite nanoparticles was clearer in anatomical detail in a larger area than iron oxide nanoparticles [36]. Results of the in vitro condition of human prostate cancer cells presented r_2/r_1 values of 59 and 50 for cobalt zinc ferrite nanoparticles coated with dimercaptosuccinic acid, respectively [37]. Moreover, the magnetization transfer contrast (MTC) technique was used with gadolinium to enhance MRI images in the brain [38].

The histogram shows a mean contrast from the MRI images of both the liver and kidney organs of the mice with 2D and 3D techniques (Figure 8). The chitosan-coated $Co_{0.5}Zn_{0.5}Fe_2O_4$ nanoparticles with 400 mT of external magnetic field assistance (red) resulted in the highest mean contrast, comparing all organs and both techniques. The mean contrast of the liver organ tended to decrease with the injection of gadolinium (pink), chitosan-coated $Co_{0.5}Zn_{0.5}Fe_2O_4$ nanoparticles without external magnetic field assistance (green), and with normal mice (black), respectively, because the gadolinium-based contrast agent infiltrated into the liver organs faster than the kidneys. However, the mean contrast of two kidneys with the chitosan-coated $Co_{0.5}Zn_{0.5}Fe_2O_4$ nanoparticles without external

magnetic field assistance (green) was higher than those for the injection of gadolinium (pink), and for normal mice (black).

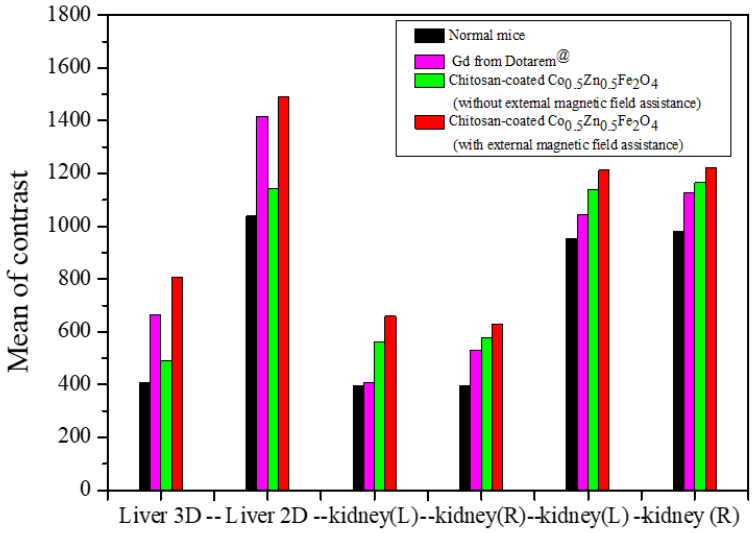


Figure 8. Mean of contrast histogram inferred from 3D and 2D MRI images of mice liver and kidneys from normal mice (black), mice injected with gadolinium (pink), mice injected with chitosan-coated $Co_{0.5}Zn_{0.5}Fe_2O_4$ nanoparticles without external magnetic field assistance (green), and mice injected with chitosan-coated $Co_{0.5}Zn_{0.5}Fe_2O_4$ nanoparticles with 400 mT of external magnetic field assistance (red).

4. Conclusions

In summary, chitosan-coated $Co_{0.5}Zn_{0.5}Fe_2O_4$ nanoparticles were successfully synthesized. The spinel phase of a cubic unit cell and small crystallite sizes of 12 nm were obtained. The core size of the chitosan-coated $Co_{0.5}Zn_{0.5}Fe_2O_4$ nanoparticles was approximately 26 ± 1.86 nm. Treating the chitosan-coated nanoparticles with a 400 mT magnetic field resulted in their magnetic properties being close to that of superparamagnetic material, as confirmed by their high M_m (8.85 emu/g) and low H_c (1.41 Oe) values. The improvement in the magnetic properties of the chitosan-coated $Co_{0.5}Zn_{0.5}Fe_2O_4$ nanoparticles is beneficial for contrast enhancement in magnetic resonance imaging. The nanoparticles were also shown to be non-toxic in the acute toxicity tests on rats. Finally, chitosan-coated $Co_{0.5}Zn_{0.5}Fe_2O_4$ nanoparticles with 400 mT of magnetic field assistance could enhance the brightness of MRI images up to 21% compared with those of gadolinium-injected mice.

Supplementary Materials: The following supporting information can be downloaded at: https://www.mdpi.com/article/10.3390/coatings13020276/s1, Video S1: MRI Measurement of 3 mice, (a) Normal mice; (b) CoZnFe2O4 with apply 400 mT; (c) CoZnFe2O4 without apply. Video S2: MRI Measurement of both mice injected with gadolinium.

Author Contributions: Conceptualization, A.W. and W.O.; methodology, A.W.; software, A.W. and W.O.; validation, A.W. and W.O.; formal analysis, A.W. and W.O.; investigation, A.W. and W.O.; resources, W.O.; data curation, A.W.; writing—original draft preparation, A.W.; writing—review and editing, A.W. and W.O.; visualization, A.W.; supervision, W.O.; project administration, W.O.; funding acquisition, W.O. All authors have read and agreed to the published version of the manuscript.

Funding: We acknowledge the financial support received from the Science Achievement Scholarship of Thailand, and the assistance of Pongsakorn Jantaratana, Faculty of Science, Department of Physics, Kasetsart University, with the VSM measurement.

Institutional Review Board Statement: The animal study protocol was approved by ethic committee name: Institute of Animals for Scientific Purposes Development (IAD) National Research Council of Thailand (NRCT), approval code: U 1-08123-2562, approval date: 27 February 2019. Wistar rats using the International Organization for Standardization (ISO 10993-11) biological evaluation of

medical devices part 11 test for systemic toxicity 2017 (ethics committee name: National Laboratory Animal Center, Mahidol University, approval code: non-GLP2019-22, approval date: 24 September 2019). $Co_{0.5}Zn_{0.5}Fe_2O_4$ nanoparticles were studied to enhance contrast agents by Intera Achieva 3 T (Philips) (ethics committee name: Advanced Diagnostic Imaging Center (AIMC), Faculty of Medicine Ramathibodi Hospital, approval code: 001/2562, approval date: 6 February 2019).

Informed Consent Statement: Not applicable.

Data Availability Statement: Not applicable.

Conflicts of Interest: The authors declare no conflict of interest.

References

1. Chan, M.H.; Li, C.H.; Chang, Y.C.; Hsiao, M. Iron-Based Ceramic Composite Nanomaterials for Magnetic Fluid Hyperthermia and Drug Delivery. *Pharmaceutics* **2022**, *14*, 2584. [CrossRef] [PubMed]
2. Darwish, M.S.A.; Kim, H.; Lee, H.; Ryu, C.; Lee, J.Y.; Yoon, J. Engineering Core-Shell Structures of Magnetic Ferrite Nanoparticles for High Hyperthermia Performance. *Nanomaterials* **2020**, *10*, 991. [CrossRef]
3. Nica, V.; Caro, C.; Páez-Muñoz, J.M.; Leal, M.P.; Garcia-Martin, M.L. Bi-Magnetic Core-Shell $CoFe_2O_4$@$MnFe_2O_4$ Nanoparticles for In Vivo Theranostics. *Nanomaterials* **2020**, *10*, 907. [CrossRef]
4. Li, L.; Jiang, W.; Luo, K.; Song, H.; Lan, F.; Wu, Y.; Gu, Z. Superparamagnetic iron oxide nanoparticles as MRI contrast agents for non-invasive stem cell labeling and tracking. *Theranostics* **2013**, *3*, 595–615. [CrossRef]
5. Bellin, M.F.; Van Der Molen, A.J. Extracellular gadolinium-based contrast media: An overview. *Eur. J. Radiol.* **2008**, *66*, 160–167. [CrossRef]
6. Khan, S.; Hossain, M.K. Classification and properties of nanoparticles. In *Nanoparticle-Based Polymer Composites*; Woodhead Publishing: Sawston, UK, 2022; pp. 15–54. [CrossRef]
7. Rubel, M.H.K.; Hossain, M.K. *Chapter: 10 Crystal Structures and Properties of Nanomagnetic Materials, Fundamentals of Low Dimensional*, 1st ed.; CRC Press: Boca Raton, FL, USA; Taylor & Francis Group: Abingdon, UK, 2022; pp. 183–205.
8. Mozaffari, M.; Manouchehri, S.; Yousefi, M.H.; Amighian, J. The effect of solution temperature on crystallite size and magnetic properties of Zn substituted Co ferrite nanoparticles. *J. Magn. Magn. Mater.* **2010**, *322*, 383–388. [CrossRef]
9. Sanpo, N.; Berndt, C.C.; Wen, C.; Wang, J. Transition metal-substituted cobalt ferrite nanoparticles for biomedical applications. *J. Acta. Biomater.* **2013**, *9*, 5830–5837. [CrossRef] [PubMed]
10. He, H.Y.; Yan, Y.; Huang, J.F.; Lu, J. Rapid photodegradation of methyl blue on magnetic $Zn_{1-x}Co_xFe_2O_4$ nanoparticles synthesis by hydrothermal process. *J. Sep. Purif. Technol.* **2014**, *136*, 36–41. [CrossRef]
11. Yadav, R.S.; Havlica, J.; Hnatko, M.; Šajgalík, P.; Alexander, C.; Palou, M.; Bartoníčková, E.; Boháč, M.; Frajkorová, F.; Masilko, J.; et al. Magnetic properties of $Co_{1-x}Zn_xFe_2O_4$ spinel ferrite nanoparticles synthesized by starch-assisted sol-gel autocombustion method and its ball milling. *J. Magn. Magn. Mater.* **2015**, *378*, 190–199. [CrossRef]
12. Samadia, M.S.; Shokrollahia, H.; Zamanianb, A. The magnetic-field-assisted synthesis of the Co-ferrite nanoparticles via reverse co-precipitation and their magnetic and structural properties. *J. Mater. Chem. Phys.* **2018**, *215*, 355–359. [CrossRef]
13. Li, Y.; Hu, K.; Chen, B.; Liang, Y.; Fan, F.; Sun, J.; Zhang, Y.; Gu, N. Fe_3O_4@PSC nanoparticle clusters with enhanced magnetic properties prepared by alternating-current magnetic field assisted co-precipitation. *Colloids Surf. A Physicochem. Eng. Asp.* **2017**, *520*, 348–354. [CrossRef]
14. Shibaev, A.V.; Shvets, P.V.; Kessel, D.E.; Kamyshinsky, R.A.; Orekhov, A.S.; Abramchuk, S.S.; Khokhlov, A.R.; Philippova, O.E. Magnetic-field-assisted synthesis of anisotropic iron oxide particles: Effect of pH. *Beilstein J. Nanotechnol.* **2020**, *11*, 1230–1241. [CrossRef]
15. Jiang, C.; Leung, C.W.; Pong, P.W.T. Magnetic-Field-Assisted Assembly of Anisotropic Superstructures by Iron Oxide Nanoparticles and Their Enhanced Magnetism. *Nanoscale Res. Lett.* **2016**, *11*, 189. [CrossRef]
16. Mohamed, W.S.; Alzaid, M.; Abdelbaky, M.S.M.; Amghouz, Z.; Granda, S.G.; Abu-Dief, A.M. Impact of Co^{2+} Substitution on Microstructure and Magnetic Properties of $Co_xZn_{1-x}Fe_2O_4$ Nanoparticles. *Nanomaterials* **2019**, *9*, 1602. [CrossRef]
17. Sattarahmady, N.; Zarea, T.; Mehdizadeh, A.R.; Azarpira, N.; Heidari, M.; Lotfi, M.; Heli, H. Dextrin-coated zinc substituted cobalt-ferrite nanoparticles as an MRI contrast agent: In vitro and in vivo imaging studies. *Colloids Surf. B Biointerfaces* **2015**, *129*, 15–20. [CrossRef]
18. Ahmad, A.; Bae, H.; Kim, C.; Rhee, I. Characterization of zinc-doped cobalt ferrite nanoparticles for application as heat generators in magnetic hyperthermia and MRI contrast agents. *J. Korean Phys. Soc.* **2019**, *74*, 1151–1159. [CrossRef]
19. Gözüak, F.; Köseoğlu, Y.; Baykal, A.; Kavas, H. Synthesis and characterization of $Co_xZn_{1-x}Fe_2O_4$ magnetic nanoparticles via a PEG-assisted route. *J. Magn. Magn. Mater.* **2009**, *321*, 2170–2177. [CrossRef]
20. Safari, R.; Hadi, H. Use of Dextran-Coated Cobalt–Zinc Ferrite Nanoparticles to Improve Image Quality in Magnetic Resonance Imaging: Non-Clinical Approach. *Russ. J. Phys. Chem. A* **2021**, *95*, 2643–2652. [CrossRef]
21. Ansari, L.; Sharifi, I.; Ghadrijan, H.; Azarpira, N.; Momeni, F.; Zamani, H.; Rasouli, N.; Mohammadi, M.; Mehdizadeh, A.; Abedi-Firouzjah, R. Synthesis, Characterization and MRI Application of Cobalt-Zinc Ferrite Nanoparticles Coated with DMSA: An In-vivo Study. *Appl. Magn. Reson.* **2021**, *52*, 33–45. [CrossRef]

22. Hossain, M.K.; Khan, M.I.; El-Denglawey, A. A review on biomedical applications, prospects, and challenges of rare earth oxides. *Appl. Mater. Today* **2021**, *24*, 101104. [CrossRef]
23. Hoque, M.D.A.; Ahmed, M.R.; Rahman, G.T.; Rahman, M.T.; Islam, M.A.; Khan, M.A.; Hossain, M.K. Fabrication and comparative study of magnetic Fe and α-Fe2O3 nanoparticles dispersed hybrid polymer (PVA+Chitosan) novel nanocomposite film. *Results Phys.* **2018**, *10*, 434–443. [CrossRef]
24. Anik, M.I.; Hossain, M.K.; Hossain, I.; Ahmed, I.; Doha, R.M. Biomedical applications of magnetic nanoparticles. In *Magnetic Nanoparticle-Based Hybrid Materials*; Woodhead Publishing: Sawston, UK, 2021; pp. 463–497. [CrossRef]
25. Indla, S.; Chelvane, A.; Lodh, A.; Das, D. Enhancement in magnetostrictive properties of cobalt ferrite by magnetic field assisted compaction technique. *J. Alloys Comp.* **2019**, *779*, 886–891. [CrossRef]
26. Coppola, P.; da Silva, F.G.; Gomide, G.; Paula, F.L.O.; Campos, A.F.C.; Perzynski, R.; Kern, C.; Depeyrot, J.; Aquino, R. Hydrothermal Synthesis of Mixed Zinc–Cobalt Ferrite Nanoparticles: Structural and Magnetic Properties. *J. Nanoparticle Res.* **2016**, *18*, 138. [CrossRef]
27. Sundararajan, M.; Kennedy, L.J.; Aruldoss, U.; Pasha, S.k.K.; Vijaya, J.J.; Dunn, S. Microwave combustion synthesis of zinc substituted nanocrystalline spinel cobalt ferrite: Structural and magnetic studies. *J. Mat. Sci. Semicon. Proc.* **2015**, *40*, 1–10. [CrossRef]
28. Yadav, R.S.; Kuřitka, I.; Havlica, J.; Hnatko, M.; Alexander, C.; Masilko, J.; Kalina, L.; Hajdúchová, M.; Rusnak, J.; Enev, V. Structural, magnetic, elastic, dielectric and electrical properties of hotpress sintered $Co_{1-x}Zn_xFe_2O_4$ (x = 0.0, 0.5) spinel ferrite nanoparticles. *J. Magn. Magn. Mater.* **2018**, *447*, 48–57. [CrossRef]
29. Shen, M.; Yu, Y.; Fan, G.; Chen, G.; Jin, Y.M.; Tang, W.; Jia, W. The synthesis and characterization of monodispersed chitosan-coated Fe_3O_4 nanoparticles via a facile one-step solvothermal process for adsorption of bovine serum albumin. *Nanoscale Res. Lett.* **2014**, *9*, 296. [CrossRef]
30. Sanpo, N.; Tharajak, J.; Li, Y.; Berndt, C.C.; Wen, C.; Wang, J. Biocompatibility of transition metal-substituted cobalt ferrite nanoparticles. *J. Nanoparticle Res.* **2014**, *16*, 2510. [CrossRef]
31. Chunpenmongkol, S.; Wantanajittikul, K.; Rerkasem, K.; Ya-in, C.; Saekho, S. Classification of carotid atherosclerotic plaque components using T2 mapping technique from magnetic resonance imaging. *J. Assoc. Med. Sci.* **2014**, *47*, 37–44. Available online: https://he01.tci-thaijo.org/index.php/bulletinAMS/article/view/59987 (accessed on 27 March 2021).
32. Xiao, Y.D.; Paudel, R.; Liu, J.; Ma, C.; Zhang, Z.S.; Zhou, S.K. MRI contrast agents: Classification and application (review). *Int. J. Mol. Med.* **2016**, *38*, 1319–1326. [CrossRef]
33. Israel, L.L.; Galstyan, A.; Holle, E.; Ljubimova, J.Y. Magnetic iron oxide nanoparticles for imaging, targeting and treatment of primary and metastatic tumors of the brain. *J. Control Release* **2020**, *320*, 45–62. [CrossRef]
34. Junior, J.E.; Santos, A.C.D.; Koenigkam-Santos, M.; Nogueira-Barbosa, M.H.; Muglia, V.F. Complications from the use of intravenous gadoliniumbased contrast agents for magnetic resonance imaging. *Radiol. Bras.* **2008**, *4*, 263–267. [CrossRef]
35. Yang, C.T.; Chandrasekharan, P.; He, T.; Poh, Z.; Raju, A.; Chuang, K.H.; Robins, E.G. An intravascular MRI contrast agent based on Gd (DO3A-Lys) for tumor angiography. *Biomaterials* **2014**, *35*, 327–336. [CrossRef] [PubMed]
36. Novotna, B.; Herynek, V.; Rossner Jr, P.; Turnovcova, K.; Jendelova, P. The effects of grafted mesenchymal stem cells labeled with iron oxide or cobalt-zinc-iron nanoparticles on the biological macromolecules of rat brain tissue extracts. *Int. J. Nanomed.* **2017**, *12*, 4519–4526. [CrossRef] [PubMed]
37. Ghasemian, Z.; Shahbazi-Gahrouei, D.; Manouchehri, S. Cobalt zinc ferrite nanoparticles as a potential magnetic resonance imaging agent: An in vitro study. *Avicenna J. Med. Biotechnol.* **2015**, *7*, 64–68. Available online: https://www.ncbi.nlm.nih.gov/pmc/articles/PMC4483316/ (accessed on 1 December 2022).
38. Elster, A.D.; Burdette, J.H. Chapter 3—Image contrast. In *Questions and Answers in Magnetic Resonance Imaging*, 2nd ed.; Mosby: St. Louis, MO, USA, 2001; p. 1272.

Disclaimer/Publisher's Note: The statements, opinions and data contained in all publications are solely those of the individual author(s) and contributor(s) and not of MDPI and/or the editor(s). MDPI and/or the editor(s) disclaim responsibility for any injury to people or property resulting from any ideas, methods, instructions or products referred to in the content.